Available online at www.sciencedirect.com
SCIENCE DIRECT
ELSEVIER
Polymer 46 (2005) 209–228
polymer
www.elsevier.com/locate/polymer

Reactive processing of polymers: effect of in situ compatibilisation on characteristics of blends of polyethylene terephthalate and ethylene-propylene rubber

S. Al-Malaika*, W. Kong

Polymer Processing and Performance Research Unit, Aston University, Aston Triangle, Birmingham B4 7ET, UK

Received 6 May 2004; received in revised form 5 August 2004; accepted 16 August 2004

Abstract

Ethylene-propylene rubber (EPR) functionalised with glycidyl methacrylate (GMA) (*f*-EPR) during melt processing in the presence of a co-monomer, such as trimethylolpropane triacrylate (Tris), was used to promote compatibilisation in blends of polyethylene terephthalate (PET) and *f*-EPR, and their characteristics were compared with those of PET/*f*-EPR reactive blends in which the *f*-EPR was functionalised with GMA via a conventional free radical melt reaction (in the absence of a co-monomer). Binary blends of PETand *f*-EPR (with two types of *f*-EPR prepared either in presence or absence of the co-monomer) with various compositions (80/20, 60/40 and 50/50 w/w%) were prepared in an internal mixer. The blends were evaluated by their rheology (from changes in torque during melt processing and blending reflecting melt viscosity, and their melt flow rate), morphology scanning electron microscopy (SEM), dynamic mechanical properties (DMA), Fourier transform infrared (FTIR) analysis, and solubility (Molau) test.

The reactive blends (PET/*f*-EPR) showed a marked increase in their melt viscosities in comparison with the corresponding physical (PET/EPR) blends (higher torque during melt blending), the extent of which depended on the amount of homopolymerised GMA (poly-GMA) present and the level of GMA grafting in the *f*-EPR. This increase was accounted for by, most probably, the occurrence of a reaction between the epoxy groups of GMA and the hydroxyl/carboxyl end groups of PET. Morphological examination by SEM showed a large improvement of phase dispersion, indicating reduced interfacial tension and compatibilisation, in both reactive blends, but with the Tris-GMA-based blends showing an even finer morphology (these blends are characterised by absence of poly-GMA and presence of higher level of grafted GMA in its *f*-EPR component by comparison to the conventional GMA-based blends). Examination of the DMA for the reactive blends at different compositions showed that in both cases there was a smaller separation between the glass transition temperatures compared to their position in the corresponding physical blends, which pointed to some interaction or chemical reaction between *f*-EPR and PET. The DMA results also showed that the shifts in the T_gs of the Tris-GMA-based blends were slightly higher than for the conventional GMA-blends. However, the overall tendency of the T_gs to approach each other in each case was found not to be significantly different (e.g. in a 60/40 ratio the former blend shifted by up to 4.5 °C in each direction whereas in the latter blend the shifts were about 3 °C). These results would suggest that in these blends the SEM and DMA analyses are probing uncorrelatable morphological details. The evidence for the formation of in situ graft copolymer between the *f*-EPR and PET during reactive blending was clearly illustrated from analysis by FTIR of the separated phases from the Tris-GMA-based reactive blends, and the positive Molau test pointed out to graft copolymerisation in the interface. A mechanism for the formation of the interfacial reaction during the reactive blending process is proposed.

Keywords: Reactive blending; Reactive processing; PET/EPR blends

1. Introduction

A cost effective approach to producing specialty materials with a new range of properties, is to combine the wide spectrum of properties that are normally only available in two or more existing polymers, by mechanical

* Corresponding author. Tel.: +44-121-359-3611; fax: +44-121-359-4094.
E-mail address: s.al-malaika@aston.ac.uk (S. Al-Malaika).

0032-3861/$ - see front matter © 2004 Elsevier Ltd. All rights reserved.
doi:10.1016/j.polymer.2004.08.050

blending, to produce a new single modified material with improved characteristics. Unfortunately, however, most polymer pairs are immiscible and when blended together would result in phase separation giving rise to poor mechanical properties and undesirable performance for target end uses. In spite of this inherent drawback, a wide range of new useful materials with improved and unique properties have been obtained from such immiscible and incompatible polymer pairs either, by the addition of a third component, usually a graft or block copolymer, or by in situ formation of such copolymers during the blend preparation. These methods result in partial compatibilisation of the otherwise incompatible polymers [1–9]. A successful compatibilisation of immiscible polymer pairs would result in the compatibiliser locating at the interface between the discrete polymer phases so it can act as an emulsifier which reduces interfacial tension and improve adhesion between the phases, thus giving rise to improved mechanical properties and overall performance. Such compatibilisation often results in stabilised morphology with fine dispersion of the second (minor) phase in the matrix, and subsequently would have a direct effect on the final properties of the blends [10,11]. Blends based on polyalkyl terephthalates (e.g. polybutylene- and polyethylene terephthalate (PBT, PET)), have been compatibilised with a range of different functionalised second polymers; examples include use of GMA-functionalised PP in PP/PBT blends [12,13], rubber toughening of PBT by maleic anhydride-grafted EPR [14], GMA-grafted EPDM for the preparation of compatibilised and dynamically vulcanised thermoplastic elastomers of PBT and EPDM [15]. It has been shown that epoxy-containing polymers are probably the best candidates as reactive compatibilisers for polyester-related blends due to the fast reactions between epoxy and carboxylic acid or hydroxyl groups.

Compatibilisation in polymer blends is usually characterised by dynamic mechanical analysis (DMA), and the viscoelastic properties (e.g. storage modulus and the damping peak, or tan δ) are known to be influenced by the microstructure of the blends [16–18]. In this study, the compatibilising effect of GMA-functionalised EPR, with PET, was investigated by examining the dynamic mechanical properties (DMA) and the morphology of these blends. The effect of two different reactive processing routes to the functionalisation of the rubber, on the blends characteristics were examined. The first was based on the conventional free radical melt grafting reaction of GMA on the rubber backbone, and the second was based on an approach we have developed in our laboratory whereby the free radical melt grafting reaction takes place in the presence of a highly reactive co-monomer, e.g. Tris [19,20]. The GMA-functionalised rubbers (*f*-EPR) produced from these two reactive processing routes resulted in polymer materials having different microstructures. The effects of variations in the microstructure produced as a result of reactive processing of the rubber with GMA in the absence and presence of a co-monomer, on the DMA and morphology of PET/*f*-EPR blends are investigated. The nature and influence of the in situ graft copolymer produced during reactive blending of PET blends containing rubber functionalised in the presence of co-monomer, on the extent of compatibilisation were also examined.

2. Experimental

2.1. Materials

Granules of Tafmar P-0480, an ethylene-propylene rubber (EPR) with a melt flow rate of 1.7 g/10 min (at 230 °C/2.16 kg), and PET (a film grade-9921W) were supplied by Mitsui Chemicals, Inc. and Eastman Chemical, respectively. Glycidyl methacrylate (GMA) (97% purity) and trimethylolpropane triacrylate (Tris) were purchased from Aldrich Chemical Co, and used as received. The peroxide (2,5-dimethyl-2,5-bis(t-butyl peroxy) hexane), T101, was kindly donated by AKZO Chemie and was used without further purification. All other chemicals and solvents were of reagent grade and were used without further purification.

2.2. Melt grafting of GMA on EPR by reactive processing methods and blending of PET with EPR-g-GMA

The peroxide-initiated melt grafting reactions of EPR with the monomer GMA in the absence (conventional reactive processing) and presence (Tris-assisted reactive processing) of the co-monomer Tris were carried out in an internal mixer (RAPRA-Hampden torque rheometer) as described before [19]. A set of GMA grafted EPR (EPR-*g*-GMA) samples having different grafting degrees and rheological properties were prepared (see Table 1).

Blends of PET and EPR (physical blends) or PET and EPR-*g*-GMA, from the different reactive processing routes described above (reactive blends) were then prepared in an internal mixer. Both polymers (PET and rubber) were initially dried before blending for more than 20 h in a vacuum oven at 135 °C (for PET) and 85 °C (for EPR). The rubber samples (EPR or EPR-*g*-GMA) were initially tumble mixed with PET (PET/EPR or PET/EPR-*g*-GMA) at different w/w ratios (50/50, 60/40 and 80/20) before melt blending in a closed chamber of the internal mixer under nitrogen at 275 °C for 10 min and a rotor speed of 65 rpm. The torque was recorded as a function of time during blending. The processed blend samples, which were cooled under nitrogen and dried in a vacuum oven at 85 °C for 24 h, were compression moulded in an electrically heated press into 2 mm thick plaques at 275 °C with 4 min pre-heating under minimum pressure followed by 30 s under a pressure of 100 kgf/cm^2. The plaques were cooled down to below 100 °C under pressure before removal from the press. For infrared analysis, thin polymer films were also compression

Table 1
EP-*g*-GMA samples used for reactive blending

Code	Composition (EP/GMA/TRIS/T101 (phr))	Processing condition (rotor speed (rpm)/temp. (°C)/time (min))	Grafting degree[a] (%)	PolyGMA formed[a] (%)	MFI (230 °C/2.16 kg)
Virgin EP	100/0/0/0	Unprocessed	0	0	1.7
G-1	100/18/0/1.0	65/190/15	1.6	3.0	0.5
G-2	100/10/0/1.0	65/190/15	1.3	1.1	0.4
TR-1	100/10/2.5/0	65/160/15	1.0	0	1.3
TR-2	100/18/2/0.194	65/190/15	2.0	0	1.1
TR-3	100/10/2.5/0.069	65/160/15	2.5	0	1.1
TR-4	100/18/2/0.097	65/160/15	3.1	0	1.2
TR-5	100/18/2/0.384	65/190/15	2.4	0	0.9
TR-6	100/10/2.5/0.114	65/190/15	2.3	0.1	0.5
TR-7	100/10/2.5/0.457	65/190/15	2.5	0.1	0.1

[a] Both grafting degree and polyGMA formed are the weight percentage contained in the modified EP.

moulded, after complete drying, into thin films (100–200 μm thick) at a temperature of 275 °C (for PET) and 150 °C (for EPR).

2.3. Melt flow index measurement, and scanning electron microscopy

The melt flow index (MFI) of the GMA-*g*-EPR samples was measured using a Davenport Melt Flow Indexer according to ASTM D1238 (230 °C and load of 2.16 kg, die $\phi = 2.095$ mm). After the samples were granulated, 3 g of each sample was charged into the barrel within 1 min. The samples were preheated for 4 min before applying the load to drive the molten polymer through the die. The time interval for the cut-offs was 1–4 min depending on the flow rate of each sample.

Morphology of all blends examined here were characterised from a cross-section of cryogenically fractured surfaces of compression moulded plaques (2 mm thick) of the samples using a Cambridge Instruments Stereoscan 90 Scanning Electron Microscope. Stripes cut from the plaques were immersed in liquid nitrogen for more than 15 min to cool down and then fractured immediately.

For better visualisation, the fractured pieces were subjected to etching using boiling toluene for 3–4 h (to extract the rubber phase from the fractured surfaces), followed by drying overnight in a vacuum oven. The dried samples were sputter-coated with gold prior to scanning electron microscopy (SEM) examination.

2.4. Measurement of dynamic mechanical properties

The DMA of PET blends were determined using a Polymer Laboratory dynamic mechanical analyser (DMA) operated at a fixed frequency of 10 Hz. All the experiments were carried out in a bending mode over the temperature range of −80 to 180 °C at a temperature ramp of 3 °C/min, using liquid nitrogen as a cryogenic medium. The dimensions of the test specimens, which were cut out from compression moulded plaques, were $50 \times 10 \times 2$ mm^3. The data were processed using a proprietary software.

2.5. FTIR analysis of PET blends

To characterise the interfacial reaction that takes place during reactive blending, a solvent extraction method was used to separate the individual components of blends of PET and EPR-*g*-GMA. The blend samples were dissolved in mixed solvents of phenol/chlorobenzene/xylene (40/40/20 w/w) followed by precipitation of the individual polymer fractions as outlined below. Fourier transform infrared (FTIR) spectra of films of the separated EPR and PET were recorded on a Nicolet FTIR Spectrometer from 4000 to 400 cm^{-1} with a 4 cm^{-1} resolution using 64 scans.

2.6. Solvent extraction procedure to separate the individual components of blends and solubility test

For solvent extraction, 1.5 g of each blend sample was dissolved into a mixed solvent of phenol/chlorobenzene/xylene (40/40/20 w/w) at 80 °C for 3–4 h. After the solution was filtered to remove any impurity, it was added to warm toluene to precipitate PET. The PET fraction was separated and the remaining solution was added to methanol to precipitate the EPR fraction. The precipitated PET and EPR fractions were dried in a vacuum oven at 80 °C for more than 20 h. About 0.1 g of the separated PET and EPR were pressed into thin films using a press at a temperature of 275 and 150 °C, respectively, and characterised by FTIR.

A solubility test, referred to as Molau test [21,22], was used with a modified solvent system to suite the blends under investigation here, as follows: 3 g sample of 80:20 w/w blends were treated with 90 ml of the mixed solvent system phenol/tetrachloroethane (60/40 w/w) at a temperature of 85–90 °C for 3–4 h. The appearance of the mixture was noted at the end of the test.

3. Results and discussion

3.1. Effect of composition of physical blends of PET/EPR on their characteristics

The characteristics and performance of compatibilised polymer blends depend on their developed morphology which, in turn, is determined by factors such as the chemical structure, viscosity of the blend components and blend composition. Before discussing the characteristics of compatibilised PET/*f*-EPR blends, the effect of the blend composition on the DMA and morphology of the corresponding physical blends (PET/EPR), processed under the same conditions, are discussed first.

DMA were measured for both the pure components (PET and EPR) and their physical blends (PET/EPR) at different compositions. The storage modulus, E', and the damping, tan δ, versus temperature curves for the individual components of the blends are shown in Fig. 1. EPR shows a glass transition temperature (T_g) peak at −24.5 °C, whereas PET has a T_g at 93.6 °C. The storage modulus, E', curve of EPR (Fig. 1(a)) shows a typical viscoelastic behaviour of an unvulcanised elastomer: a high modulus below its T_g followed by a drastic drop by 2 orders of magnitude around the glass transition zone. By contrast, changes in the storage modulus of PET (see Fig. 1(b)) are less severe around the glass transition zone because of its semi-crystalline nature; the increase in the modulus observed around 100 °C is, almost certainly, due to crystalisation of PET during annealing.

Fig. 2 shows the tan δ curves for the physical blends of PET/EPR. Blends with different compositions having ratios of 80/20 and 60/40 w/w show two distinct and clearly

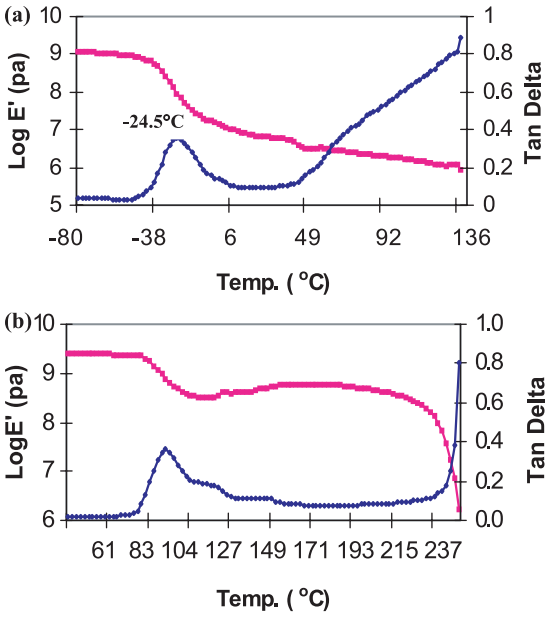

Fig. 1. DMA curves (E' and Tan δ as function of temperature) for (a) EPR and (b) PET.

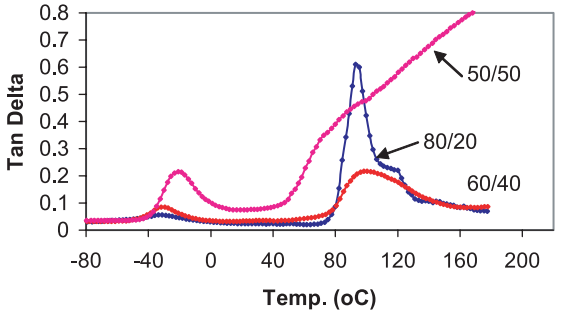

Fig. 2. Tan δ curves as function of temperature for different compositions (numbers on curves are w/w ratios) of physical blends of PET/EPR.

separated tan δ peaks corresponding to T_gs of the components, PET and EPR, see also Table 2, typical of incompatible blends [23]. In the case of the 50/50 w/w blend, on the other hand, only one tan δ peak is observed at −21 °C corresponding to the T_g of the rubber. Although no distinct peak is observed for the PET component, the tan δ curve shows a progressive increase at temperature above 50 °C which overlaps the glass transition zone of PET. The pronounced difference observed in the tan δ curve in this case is, most likely, due to the rubber component undergoing a phase inversion and changing from being dispersed to becoming the continuous phase. The data in Table 2 show clearly that the peak positions of tan δ vary with blend composition; for example at higher rubber content, the tan δ peak corresponding to EPR shifts to higher temperatures, see also Fig. 3. The dependence of tan δ peak on weight ratios of the individual polymer components in other blends based on different polymer combinations has been reported previously [17,24,25] and has been shown to relate to differences in blend morphology.

Examination of the morphology of the physical blends reveals that for blends containing 20% EPR, the rubber phase is dispersed as spherical particles (observed as semi-spherical holes after etching by hot toluene to remove the EPR phase) in the continuous PET matrix (Fig. 4(a)).

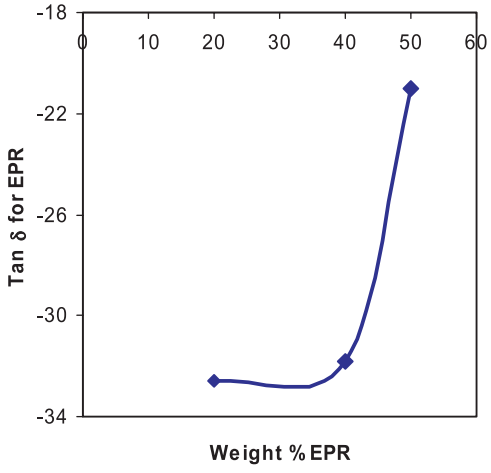

Fig. 3. Changes in tan δ of EPR phase in PET/EPR physical blends having different weight ratios of EPR.

Table 2
Damping peaks from tan δ curves corresponding to the glass transition of individual component for different types of blends of PET/EPR (or EPR-*g*-GMA)

Blends ratio, w/w PET/EPR or PET/EPR-*g*-GMA	Physical blends		Compatibilised blends							
	PET/EPR		PET/EPR-*g*-GMA_{T101}[a] (PET/G-2)				PET/EPR-*g*-GMA_{TRIS}[b] (PET/TR3)			
	EPR phase	PET phase	EPR phase		PET phase		EPR phase		PET phase	
	T_g (°C)	T_g (°C)	T_g (°C)	Shift (°C)	$T_{g\text{-PET}}$ (°C)	Shift (°C)	T_g (°C)	Shift (°C)	T_g (°C)	Shift (°C)
100/0	–	93.6	–	–	93.6	–	–	–	93.6	–
80/20	−32.6	94.1	−33.2	−0.6	89.6	−4.5	−32.1	+0.5	88.6	−5.5
60/40	−31.8	98	−29.2	+2.6	95.4	−2.6	−27.3	+4.5	94.1	−3.9
50/50	−21.0	–	−23.2	−2.2	87.2	–	−18.6	+2.4	91.7	–
0/100	−24.5	–	−22.5	+2	–	–	−22.4	+2.1	–	–

[a] EPR-*g*-GMA_{T101}—sample G-2.
[b] EPR-*g*-GMA_{TRIS}—sample TR-3.

Increasing the rubber content from 20 to 40% maintains the rubber as the dispersed phase, but with a notable difference in its characteristics showing a significant increase in its size and size distribution (Fig. 4(b)); this may be attributed to the re-agglomeration or coalescence of the dispersed rubber particles. Further, the SEM micrographs of these physical blends show a clear two phase morphology with the rubber particles being coarsely dispersed in the continuous PET phase and having clear and sharp interfacial boundaries which may be attributed to high interfacial tension indicating poor adhesion at phase boundaries, and is a manifestation of the incompatibility of the polymer components in these blends. It is well known that blends based on immiscible polymer pairs are characterized by great interfacial tension which makes the dispersion during the blending operation difficult, and contributes to unstable morphology (coalescence of phases) and poor adhesion [12,17,26].

3.2. Effect of microstructure of GMA-functionalised rubber (f-EPR) on the extent of compatibilisation of binary PET/f-EPR blends

We have shown recently [19] that functionalisation of

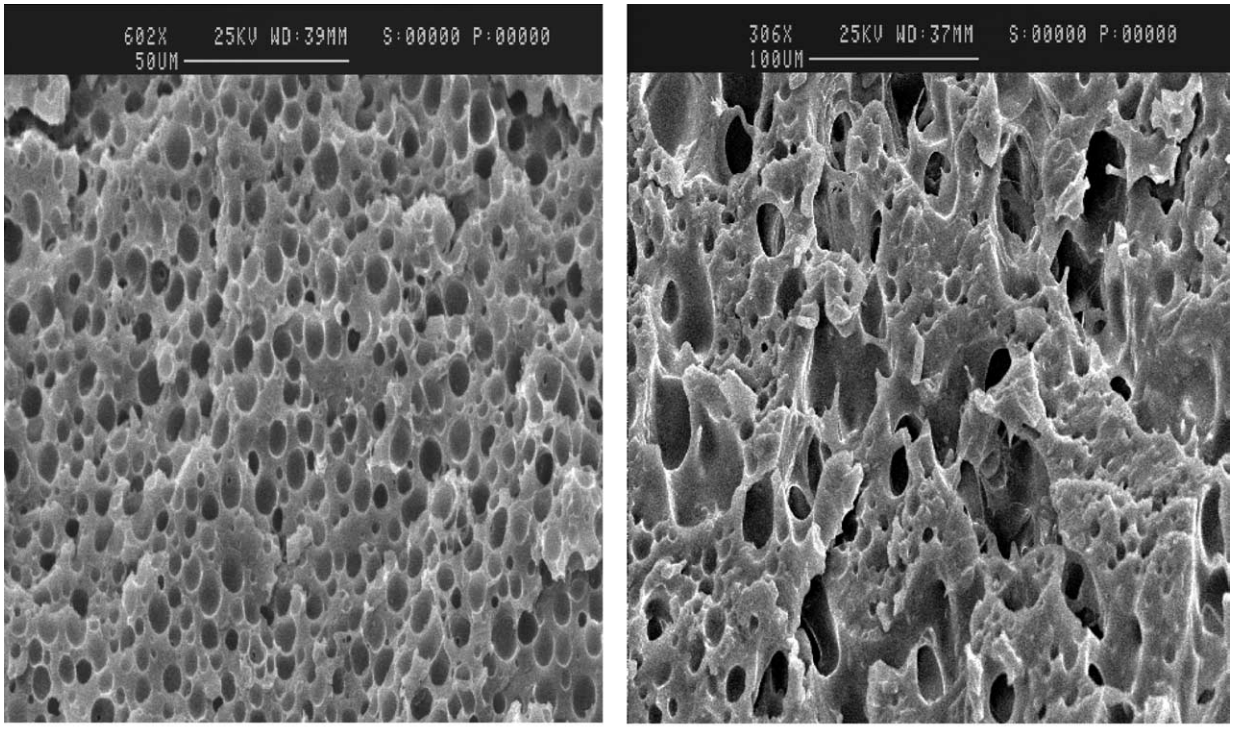

(a) PET/EPR 80:20 w/w **(b) PET/EPR 60:40 w/w**

Fig. 4. SEM micrographs of physical blends of PET/EPR having different weight ratio compositions.

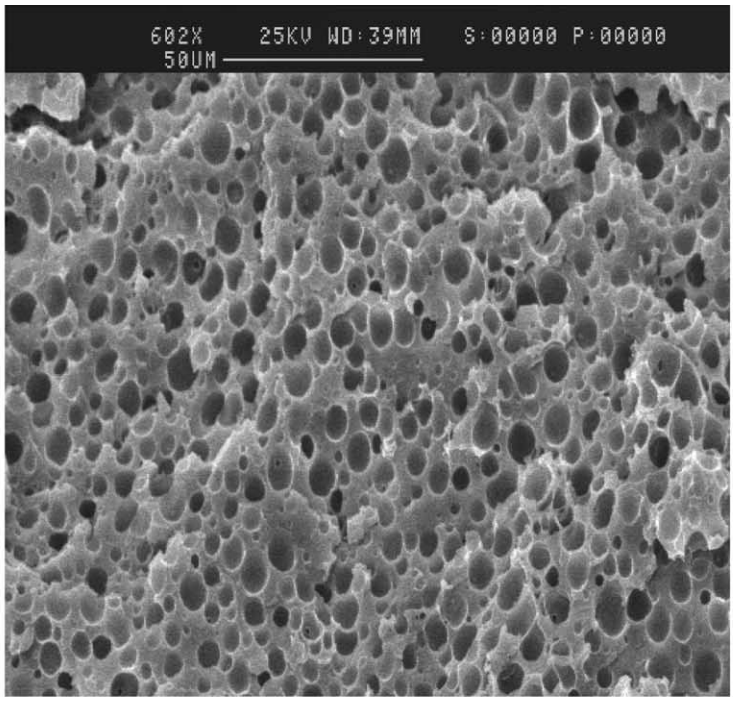

(a) PET/EP Physical Blend, 80:20 w/w

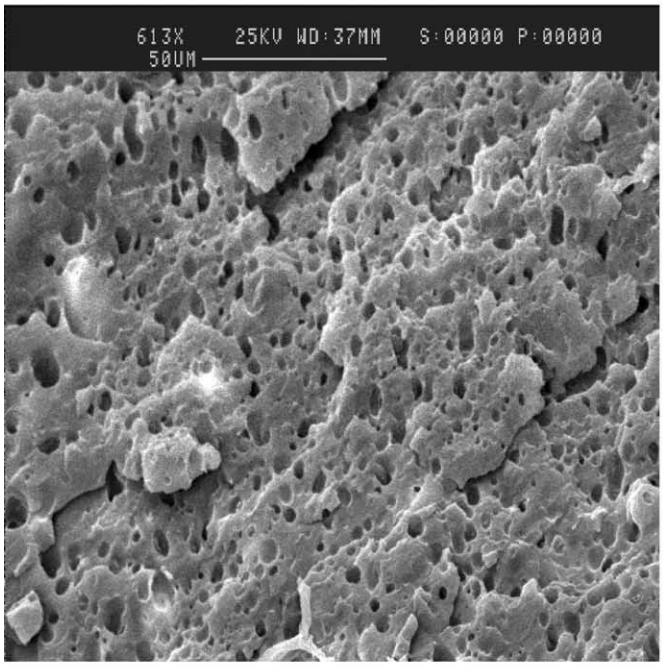

(b) PET/EP-g-GMA$_{T101}$ - Unpurified
g-GMA=1.6% , **PolyGMA=3%**

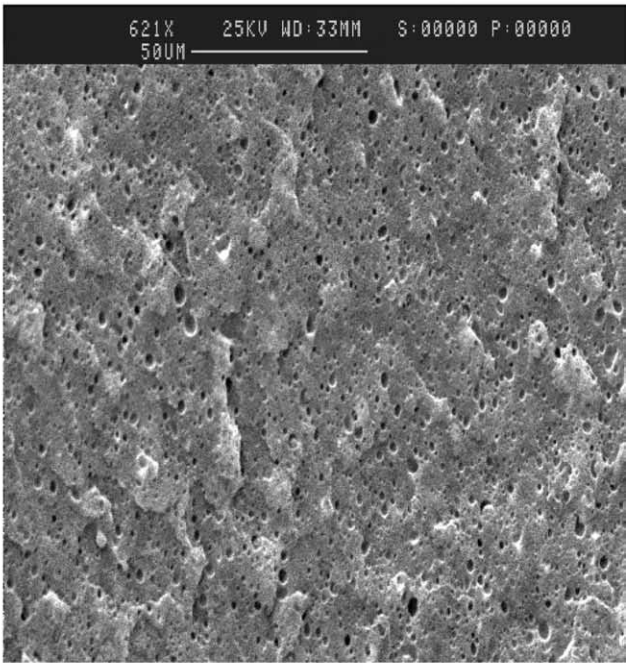

(c) PET/EP-g-GMA - Purified
g-GMA=1.6% , **PolyGMA = 0%**

Fig. 5. SEM micrographs of 80/20 w/w PET/EP-*g*-GMA$_{T101}$ blends. The rubber in the blends is based on sample G1 which was used either without or with purification (the latter to remove poly-GMA) before blending with PET.

EPR with the reactive monomer GMA, using conventional peroxide-initiated melt grafting reactions (samples identified as EPR-*g*-GMA$_{T101}$) gives rise to high amount of poly-GMA (homopolymerisation of GMA constitutes the main competing reaction). High levels of grafting could only be achieved by this method when high concentrations of the peroxide and the GMA were used. Further, this approach was shown to result in a significant increase in the viscosity of the modified polymer, due to crosslinking, when compared to the virgin (unmodified) EPR. On the other hand, when the free radical grafting reaction of GMA on EPR was conducted in the presence of a reactive

multifunctional co-monomer, e.g. Tris, (samples referred to as ERP-*g*-GMA_{TRIS}), a much higher GMA grafting level was obtained with no measurable amount of poly-GMA formed and with less change to the rheological characteristics of the modified polymer, in comparison to the unmodified analogue, with a much lower peroxide concentration needed here to achieve the optimum grafting reaction [19]. The effect of the different microstructures formed as a result of preparing the functionalised rubber samples with different chemical compositions (by the two different reactive processing approaches described above) on the extent of compatibilisation of binary blends of PET/*f*-EPR in terms of their morphology and DMA were investigated.

3.2.1. Effect of amount of poly-GMA formed in the f-EPR

Modification of EPR with GMA by conventional reactive processing (EPR-*g*-GMA_{T101}) was shown to result in the formation of poly-GMA, alongside the grafted GMA, under all conditions examined [19].

To investigate the effect of poly-GMA on the dispersion of the rubber phase in the PET matrix, one sample of EPR-*g*-GMA_{T101} was prepared by a conventional reactive processing route, in which the poly-GMA concentration formed was 3% and the degree of grafting was 1.6% (sample G-1 in Table 1). Part of this sample was purified to remove the poly-GMA (leaving a polymer containing grafted GMA only) using a solvent extraction and precipitation procedure described previously [19]. Both the unpurified and purified samples were then blended with PET at a ratio of 80/20 w/w using the same blending conditions. Examination of SEM of these blends, Fig. 5, shows that, while the physical blend is characterized by a coarse dispersion of the rubber phase with clear well defined and sharp boundaries typical of incompatibility, the reactive blends give rise clearly to reduced average particle size resulting in finer dispersion, pointing out to reduced interfacial tension due, almost certainly, to the formation of an in situ graft copolymer that locates at the interface (see Section 3.4 later). It is generally known [4,18,27] that graft copolymers formed in situ act as compatibilisers for otherwise incompatible polymer blends, and such compatibilisers contribute to reducing interfacial tension and the tendency of the dispersed particles to coalesce, thus resulting in improved dispersion during processing giving rise to reduced average size of the dispersed particles. However, the amount of poly-GMA present in the rubber phase of these blends seem to affect the extent of compatibilisation achieved. Compared to the unpurified sample (containing poly-GMA), the purified analogue (in which all formed poly-GMA had been removed) shows an even more reduction in the domain size resulting in very fine dispersion. It has been shown [27] that the particle size of a rubber dispersed phase in PET matrix is directly proportional to the interfacial tension. This would support the view that the absence of poly-GMA in these blends, which results in finer dispersion of the *f*-EPR particles, would result in a reduced interfacial tension thus contributing to the enhancement of compatibilisation. The adverse effect of poly-GMA on the dispersion of the rubber phase in the PET matrix may be attributed to further reactions of the epoxy groups in poly-GMA (in addition to reactions from grafted GMA) with the end (–COOH, –OH) groups in PET leading to the formation of branched *f*-EPR-*co*-PET copolymer which may not be necessarily located at the interface and would not, therefore, necessarily improve the compatibility between the blended polymers.

Examination of the torque–time curves developed during the reactive blending process for blends containing purified (no poly-GMA) and unpurified (3% poly-GMA) rubber samples lends support to a mechanism involving branching/crosslinking reactions as suggested above. It can be seen from Fig. 6 that the torque curve for the unpurified PET/EPR-*g*-GMA_{T101} blend is higher than that of the corresponding purified sample confirming a higher viscosity of this blend. To illustrate further the occurrence of the branching reaction between poly-GMA and PET, the PET was processed alone (in the absence) and in the presence of 4% synthesised poly-GMA using the same condition as those employed during the blending of PET with the functionalised rubber samples. It is clear from Fig. 6 that for PET, the torque decreased rapidly in the first 2–3 min dropping afterwards to a steady low value of 7 Nm. However, when PET was processed in the presence of added poly-GMA, an initial increase in the torque was observed in the first 2–3 min followed by a steady decrease to a much higher final value of 18 Nm; the overall torque curve is much higher than that of the PET processed alone. It has been suggested [4] that an increase in torque (which corresponds to increase in melt viscosity) during mixing, is an indication of reactions taking place between the polymers. The higher torque values observed in the presence of poly-GMA (see Fig. 6), adds further support to the mechanism suggested which involves branching and/or crosslinking reactions between the epoxy groups of the poly-GMA and end groups in the PET matrix during melt processing, and would explain the melt viscosity differences between the two polymers in the blends. It has been shown [27] that when the viscosity of the two phases of blends are matched, or only slightly different, there would be a minimum interfacial tension concomitant with the dispersed phase forming the smallest average particles size. Consequently, the larger particle size and coarser dispersion observed for this sample (see Fig. 5) are tentatively attributed to the unfavourable melt viscosity difference in the blend sample containing poly-GMA.

The discussion above suggests that it is critical to adopt reactive processing routes for the functionalisation of polymers that would result in a good degree of grafting of functional monomers such as GMA, but without, or with minimum formation of the corresponding homopolymer, e.g. poly-GMA, in order to ensure a higher extent of compatibilisation between the rubber phase and the matrix. To illustrate this, we have examined the morphology of two

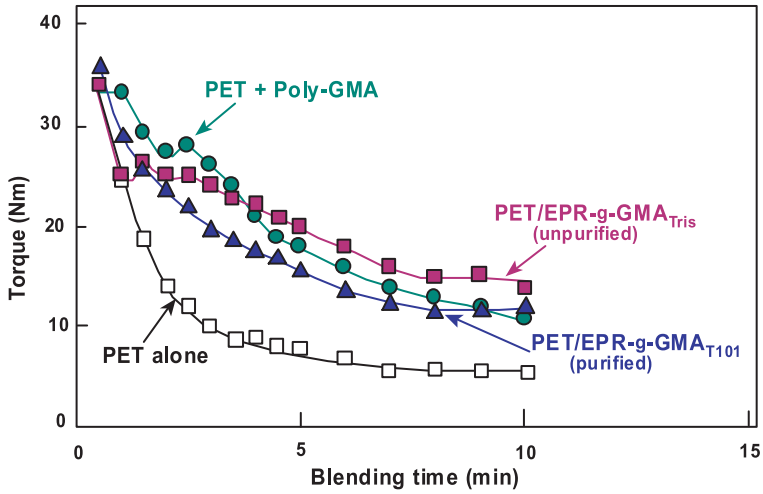

Fig. 6. Torque–time curves developed during blending PET with EP-*g*-GMA$_{T101}$ (unpurified containing grafted GMA and 3% poly-GMA, and purified where all poly-GMA was removed) at a weight ratio of 80/20. Torque curves for melt processed PET alone and PET mixed with synthesized poly-GMA are also shown.

PET/EPR-*g*-GMA blends in which the functionalised rubbers were produced by two different reactive processing routes. In the first rubber sample a conventional reactive processing procedure was used in the presence of a peroxide to produce GMA-functionalised rubber containing about 1% poly-GMA (EPR-*g*-GMA$_{T101}$: sample G-2) and for the second sample, a highly reactive co-monomer was used in the presence of a much smaller peroxide concentration to produce a GMA-functionalised rubber containing no poly-GMA (EPR-*g*-GMA$_{Tris}$: sample TR-4, see Table 1). Examination of Fig. 7 shows that the morphology of these two blend samples (blended at weight ratio of 60:40 of the PET: EPR-*g*-GMA) is very different. The blend containing poly-GMA (and lower degree of grafting) shows a clear and smooth interfacial boundaries at the rubber/matrix interface (see micrograph b, Fig. 7), whereas the one without poly-GMA (and a higher level of g-GMA) shows a much rougher interfacial boundaries which could suggest a higher degree of compatibilisation.

3.2.2. *Effect of the degree of GMA grafting*

The degree of GMA-grafting in the rubber phase should play an important role in achieving the required level of compatibilisation of the blends via in situ interfacial reactions that occur between the epoxide groups (in the functionalised rubber) and the end groups in the PET matrix during the reactive blending process. We have therefore examined the influence of functionalised rubber, and in particular, the effect of the level of GMA grafting in the rubber phase, on the morphology and rubber particle dispersion in PET/EPR-*g*-GMA blends. Fig. 8 shows scanning electron micrographs of different blends of PET/EPR-*g*-GMA$_{Tris}$ (80:20 w/w) processed under the same conditions with their rubber phase having similar melt viscosity (MFI about 1 g/10 min) and similar torque/time curves during their processing, but containing different levels of grafted GMA. At grafting level of 1%, a demonstrable reduction in the dispersed rubber domain size, compared to the physical blend, (Fig. 8(b)) is clearly evident. A further increase in the degree of grafting up to 3% results in more reduction in the domain size (Fig. 8(c)) of the rubber phase, suggesting that, in this system, a higher level of grafting contributes to the formation of finer particle size and size distribution, and this is expected to be directly proportional to a reduced interfacial tension and better extent of compatibilisation [27]; although the relationship between this and the level of GMA-grafting has not been established, the optimum level is thought to be near 2.5–3%.

3.2.3. *Effect of viscosity ratio of the blend components*

The viscosity of the rubber component in blends is one of the important factors that controls the dispersion of the rubber phase in the polymer matrix. The main mechanism governing the morphology development in blends is believed to be the result of both droplet breakup and coalescence. It has been mentioned earlier [27] that a minimum particle size is achieved when the viscosities of the two phases of the blends are closely matched. In the case of PET/EPR blend systems, the rubber component has a higher viscosity than the PET component. Although the viscosity of the polymers were not measured directly by, for example, capillary rheometry, the torque/time curves obtained in real-time during processing in the batch mixer were used to follow changes in melt viscosity; higher torque values corresponding to higher melt viscosities. Thus, the difference in the viscosities of the EPR and PET (individual polymers) is clearly evident from the observed differences in their torque/time curves: EPR has much higher torque values than PET, see Fig. 9. It was mentioned earlier (Section 3.2.1) that any factor contributing to a further increase in the viscosity of the rubber, would result in an even larger difference in the viscosities of the two phases

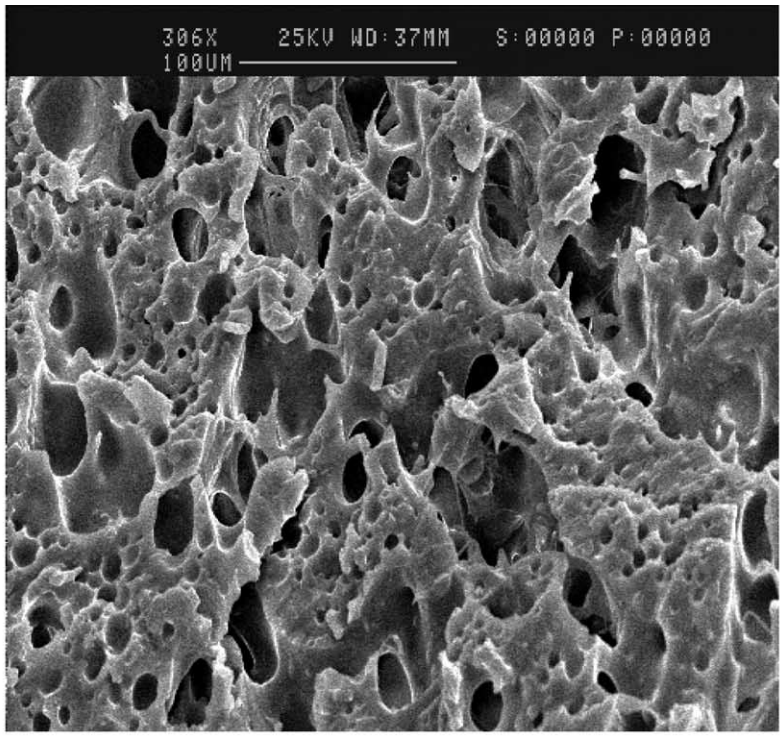

(a) PET/EP Physical Blend 60: 40

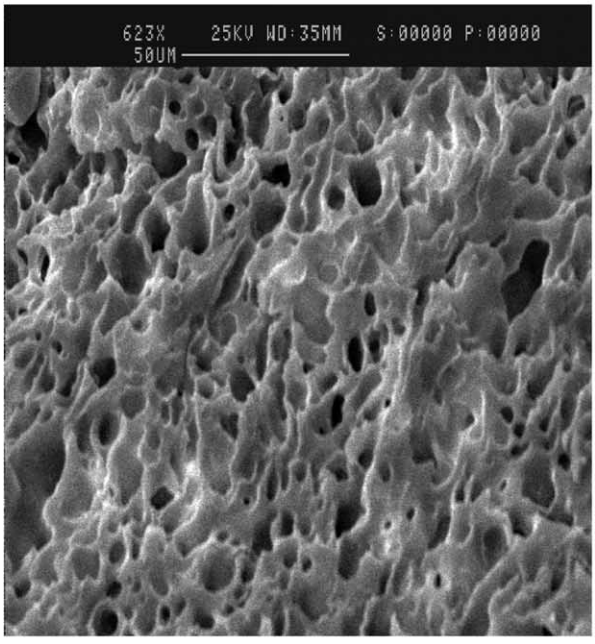

(b) PET/EP-g-GMA$_{T101}$

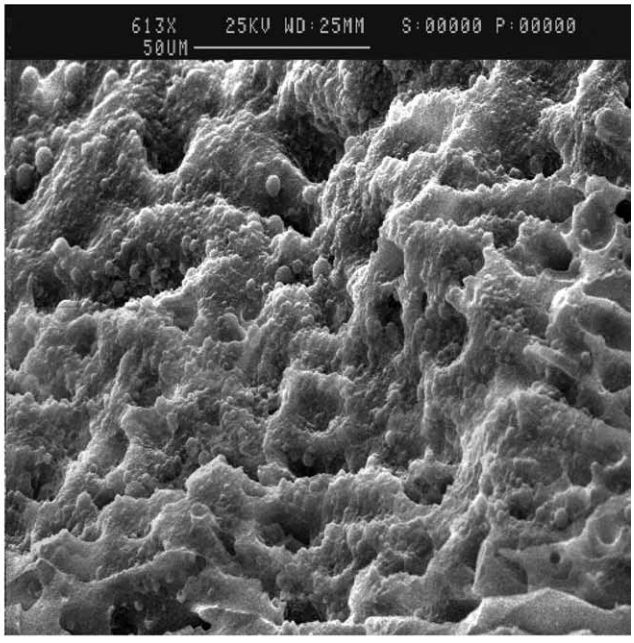

(c) PET/EP-g-GMA$_{Tris}$

Fig. 7. SEM micrographs of 60/40 w/w PET/EP-*g*-GMA blends. (b) The functionalised rubber in this blend is based on sample G2. (c) The functionalised rubber is based on sample TR4.

with adverse effects. To illustrate this, the morphologies of different PET/*f*-EPR (EPR-*g*-GMA$_{Tris}$ and 80:20 w/w) reactive blends were examined. These blends, which were processed under the same conditions, contain *f*-EPR having similar grafting level (about 2.5%) but different torque/time curve heights, see Fig. 10, indicating different melt viscosities. The difference in melt viscosities is further supported by the different MFI values obtained, ranging from 0.1 to 0.9 g/10 min (the latter value is for sample TR5 which has the lowest torque values and with a torque/time

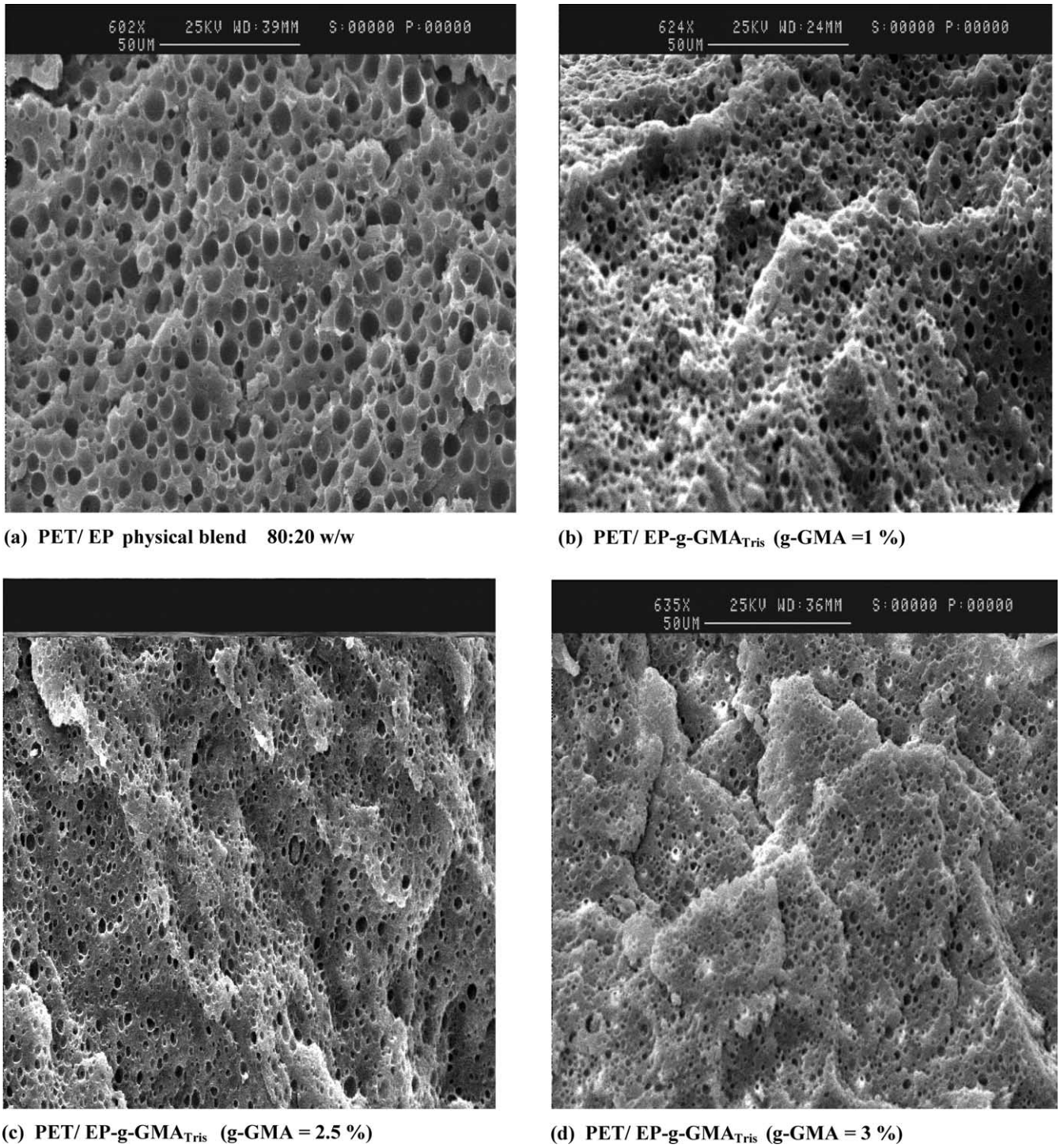

(a) PET/ EP physical blend 80:20 w/w

(b) PET/ EP-g-GMA$_{Tris}$ (g-GMA =1 %)

(c) PET/ EP-g-GMA$_{Tris}$ (g-GMA = 2.5 %)

(d) PET/ EP-g-GMA$_{Tris}$ (g-GMA = 3 %)

Fig. 8. SEM micrographs of 80/20 w/w ratio PET/EP-*g*-GMA blends. (a) Physical blend; the functionalised rubber in the blend is (b) sample TR-1, (c) sample TR-3 and (d) sample TR-4.

curve quite similar to that of the unmodified EPR), see samples TR-5, TR-6 and TR-7 in Table 1. It is clear from examination of the morphology of these samples (see Fig. 11) that blends containing *f*-EPR with higher melt viscosity (e.g. sample TR7 with lowest MFI and highest torque values, Fig. 11(a)) show rubber particles of larger domain size than those obtained with lower viscosity (see Fig. 11(c)). This confirms that in these PET-*f*-EPR binary blends, the larger the difference in the melt viscosities of the individual components (reflected from the lower MFI and higher torque values compared to the corresponding unmodified EPR), the more difficult it becomes for the higher viscosity *f*-EPR phase to disperse in the lower viscosity PET polymer matrix, thus contributing to

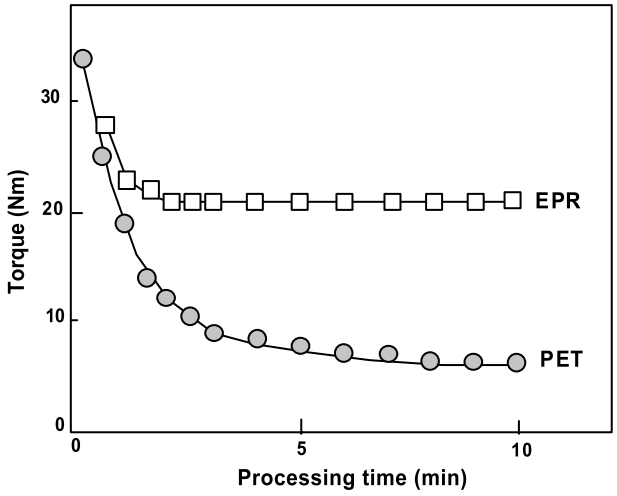

Fig. 9. Torque–time curves of PET and EPR polymers (each processed separately).

increasing interfacial tension between the phases and the observed larger *f*-EPR particle size.

3.3. Effect of functionalisation of EPR (f-EPR) in the absence and presence of a co-monomer on PET/f-EPR blends characteristics and compatibilisation

Reactive functionalisation of EPR with GMA using a conventional (peroxide-initiated but without a co-monomer) and a co-monomer (Tris)-assisted reactive processing approaches was shown to result in EPR-*g*-GMA with very different microstructures and characteristics [19]. In an attempt to investigate the differences that these methods of rubber functionalisation may have on the characteristics and extent of compatibilisation of blends with PET, we have examined both the dynamic mechanical (DMA) properties and the morphology of such blends (conventional-GMA reactive blends PET/EPR-*g*-GMA_{101} and Tris-GMA reactive blends, PET/EPR-*g*-GMA_{Tris}) having different compositions (weight ratios of 50:50, 60:40 and 80:20). Fig. 12 shows the DMA curves for 50:50 w/w ratio functionalised rubber-containing blends, and that of the corresponding physical blend. It is clear that while the tan δ curve of the physical blend shows only one peak that corresponds to EPR, in the case of both the functionalised rubber-containing blends, two separate peaks were observed corresponding to the glass transition temperatures of PET and EPR, which are clearly shifted to lower temperatures. For partially compatible blends, it is expected to see a shift in the glass transition temperatures of the component polymers as well as some broadening of the transition peaks [17].

Closer examination of Fig. 12 shows that the tan δ peak of the rubber phase in the conventional-GMA reactive blend (PET/EPR-*g*-GMA_{T101}) is shifted to a lower (-2.2 °C) temperature (the shift is relative to the T_g of the corresponding physical blend), whereas the rubber phase peak in the Tris-GMA blend (PET/EPR-*g*-GMA_{TRIS}) became broad and shifted to a higher temperature, i.e. moved closer to the PET transition temperature by $+2.4$ °C, see Table 2. Since the physical blend at this weight ratio did not show a clear T_g for the PET phase, no temperature shift could be determined in the PET region, however, the difference in the tan δ peak values of PET phase in each of the two blends (87.2 and 91.7 °C for conventional-GMA and Tris-GMA blends, respectively) may reflect a difference in the phase structure of these blends. In the case of PET/EPR-*g*-GMA_{T101} blend, the PET is most likely still the continuous phase as indicated by a 'normal shape' of its tan δ peak and the steady value of the storage modulus (E') within the temperature range 0–80 °C, whereas the shapes of the tan δ and E' curves of the PET/EPR-*g*-GMA_{TRIS} blend, suggests that the PET forms possibly a co-continuous phase.

Decreasing the amount of the rubber in the physical blend from 50 to 40% results clearly in two distinct damping peaks corresponding to glass transition temperatures of the rubber (at -31.8 °C) and PET matrix (at 98 °C), see Fig. 13.

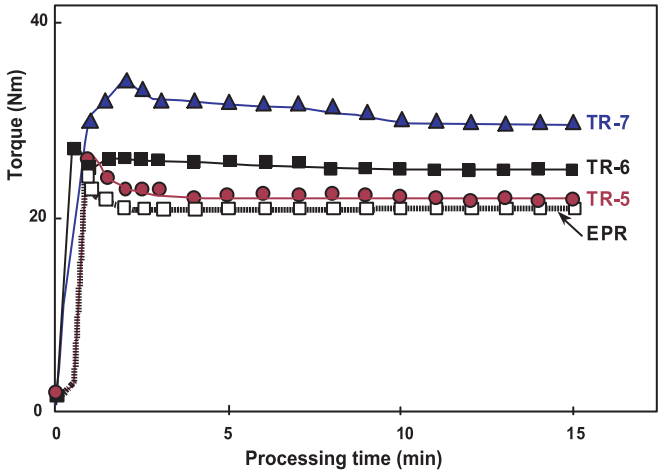

Fig. 10. Torque–time curves during blending of reactive blends of various *f*-EPR (EPR-*g*-GMA_{Tris}) compared to that of EPR; all samples were produced under the same melt processing conditions.

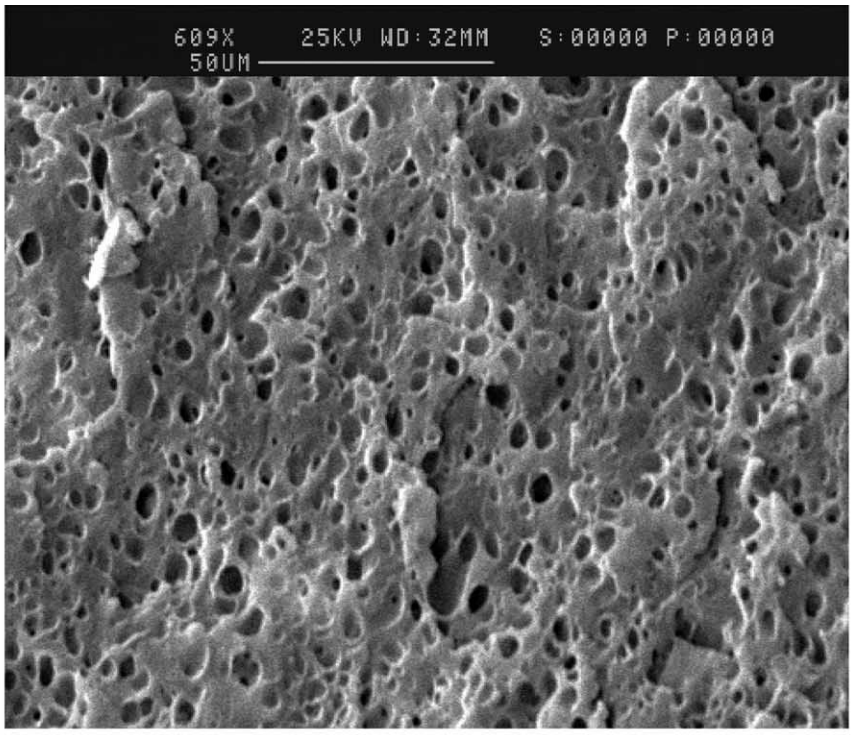

(a) PET/EPR-g-GMA$_{Bris}$ TR-7 MFI=0.1 (highest viscosity ratio)

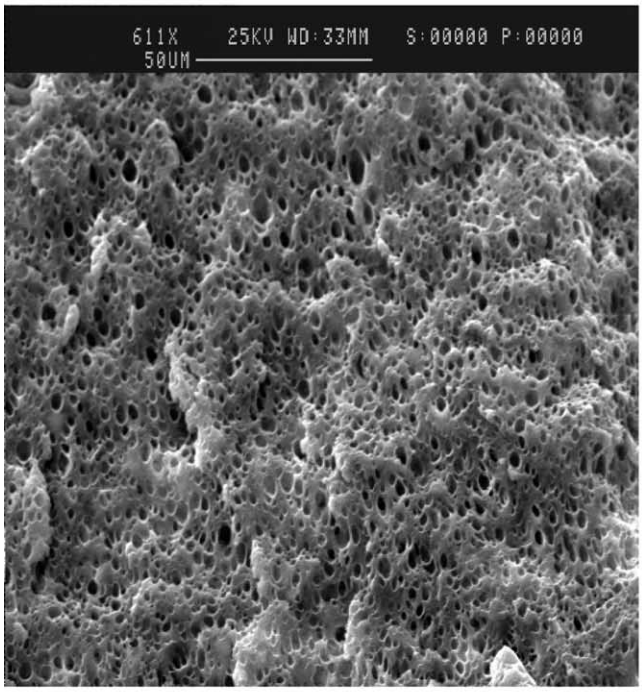

(b) PET/EPR-g-GMA$_{Tris}$, TR-6, MFI=0.5

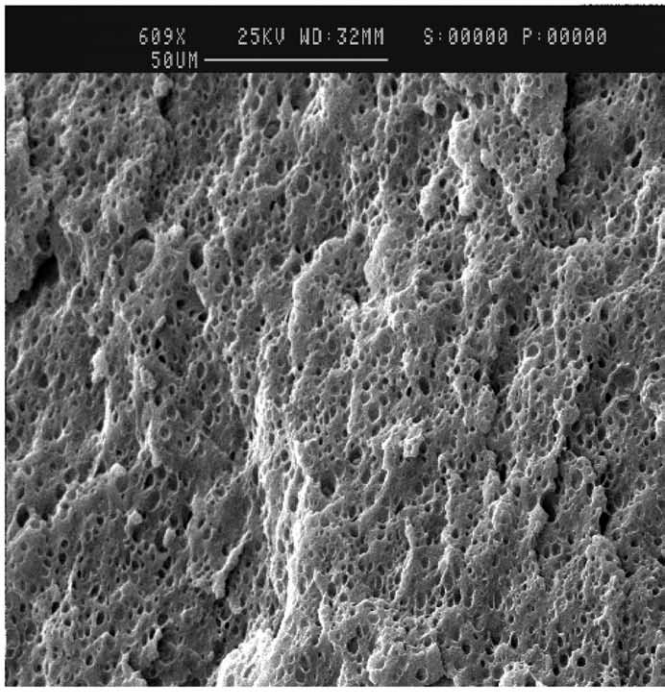

(c) PET/EPR-g-GMA$_{Tris}$, TR-5, MFI=0.9

Fig. 11. SEM micrographs of 80/20 w/w ratio PET/EP-*g*-GMA$_{Tris}$ blends having similar level of GMA grafting but different viscosities (different MFI values) of their modified rubber phase, samples TR-5 to TR-7.

As in the case of the 50:50 w/w composition, the 60:40 w/w reactive PET/EPR-*g*-GMA blends (conventional and Tris-GMA) also show two tan δ peaks which do not remain at their original positions but undergo a clear temperature shift. Fig. 14 shows the extent of shifts in the glass transition temperatures relative to the corresponding physical blend (from DMA data) for these two reactive blends; it also shows that in both cases, the T_g of the *f*-EPR phase shifts to higher temperatures, whereas the T_g of the PET phase shifts to lower temperatures, i.e. the glass transition temperatures

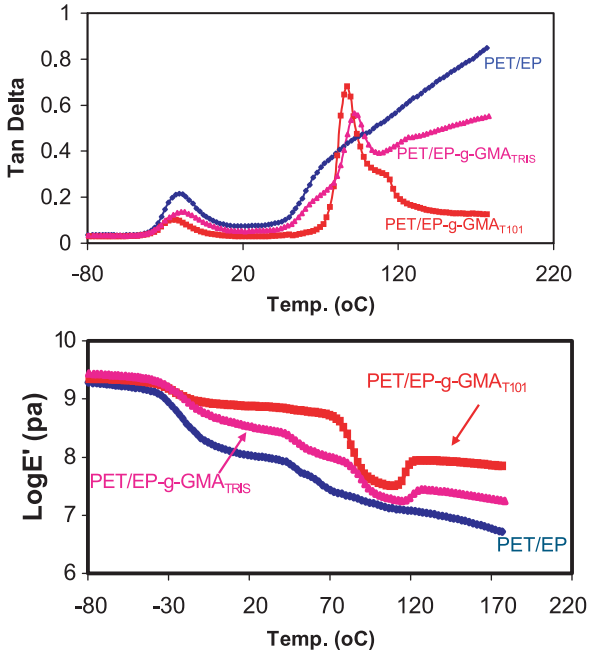

Fig. 12. DMA curves for physical (PET/EPR) and functionalised (PET/EP-*g*-GMA) blends (50/50 w/w) as a function of tan δ and E'.

of the two phases shift closer towards each other, with the Tris-GMA blend showing a slightly higher extent of the shift in its T_g of both phases. DMA technique is known to be sensitive to detection of transitions and disturbances caused by chemical reactions and interactions between the phases of reactive blends [21] and T_g values of partially compatible

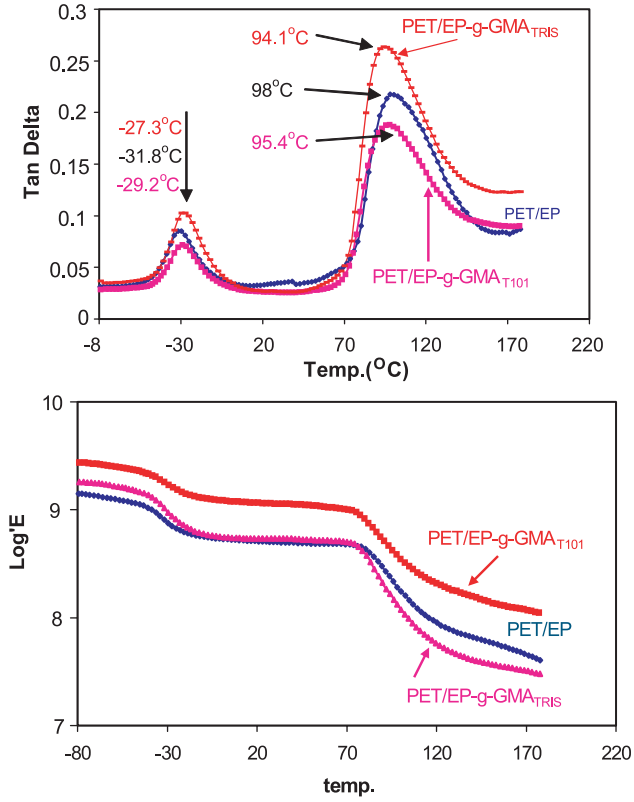

Fig. 13. DMA curves for PET/EP-*g*-GMA blends (60/40 w/w) as a function of Tan δ and E'.

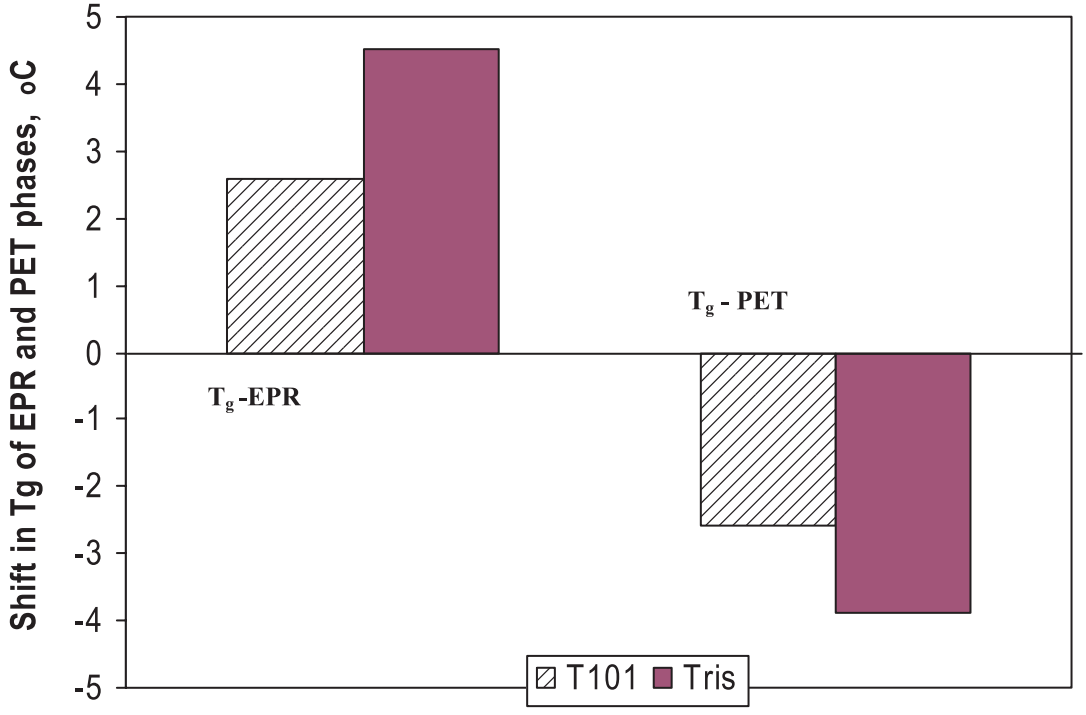

Fig. 14. The extent of shift in T_g (relative to that of corresponding physical blend; taken from tan δ of DMA curves) for each of the rubber and the PET phases in reactive blends (60:40 w/w). Hashed areas represent conventional-GMA blend (PET/EPR-*g*-GMA$_{T101}$) and solid blocks are for the Tris-GMA blend (PET/EPR-*g*-GMA$_{Tris}$).

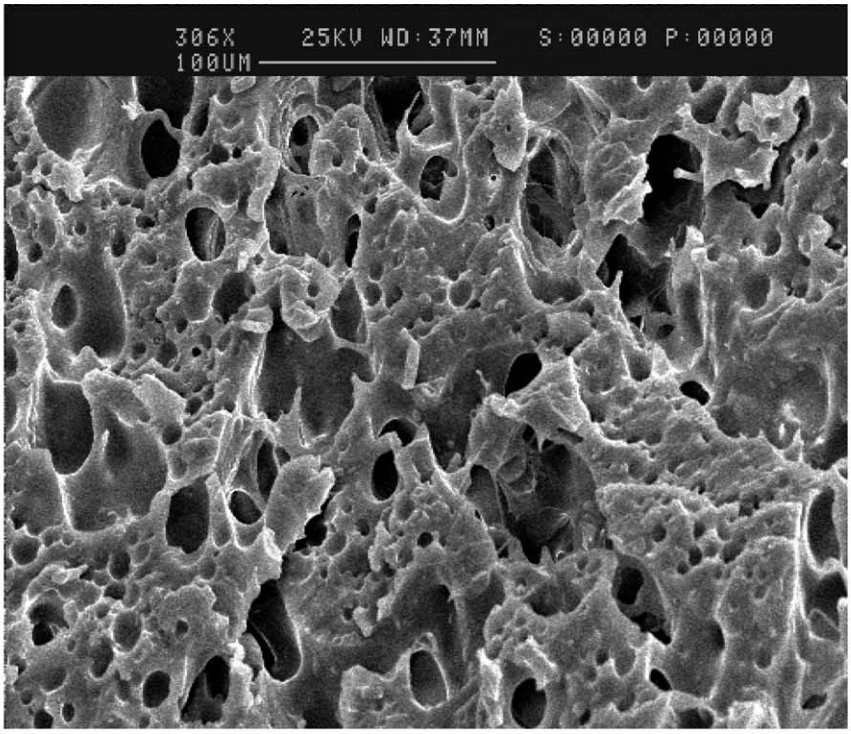

(a) PET/EPR 60:40 w/w Physical Blend

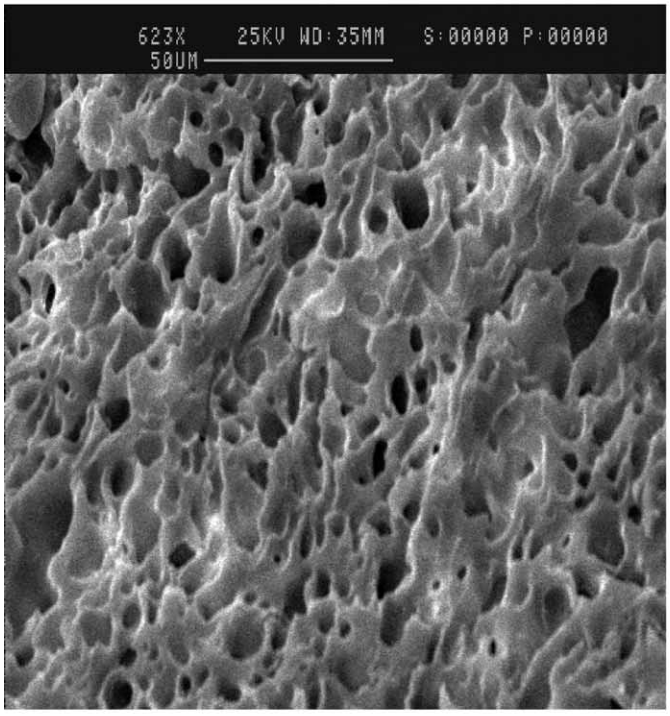

(b) PET/EPR-g-GMA$_{T101}$

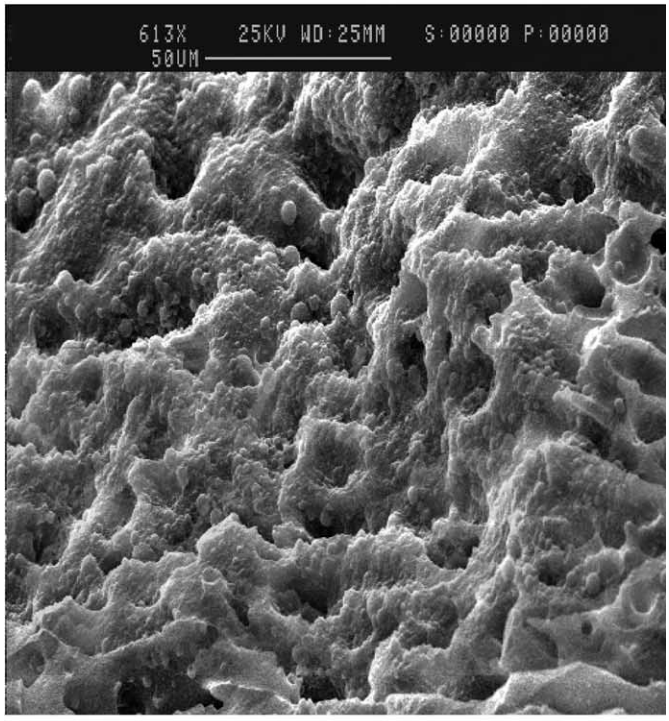

(c) PET/EPR-g-GMA$_{Tris}$

Fig. 15. SEM micrographs of 60/40 w/w ratio physical (note the different scale) and reactive blends. The functionalised rubber in (b) is based on sample G2 whereas in (c) the functionalised rubber is based on sample TR-3.

blends are known to shift towards each other [18]. The clear shift in the T_gs (by up to 4.5 °C in the case of Tris-GMA blend) is a good indication that both reactive blends have undergone compatibilisation via in situ chemical reactions between the two phases during the melt blending, resulting in the formation of a copolymer at the interface that is able to act as an emulsifier and promote compatibilisation of the phases. However, it is difficult, though tempting, to

conclude from these DMA results that the Tris-GMA blend offers higher extent of compatibilisation compared to the conventional blend, albeit the extent of the T_g shifts in the case of the former is slightly greater than that for the latter, in view of the width of the glass transition region, and the fact that the two *f*-EPR components of the blends were produced by two different reactive processing routes (blends with EPR functionalised in presence or absence of the co-monomer Tris). Fig. 14 supports this conclusion and shows that the tendency for the separate glass transition temperatures to approach each other is, in fact, not very different in each case (i.e. in presence and absence of Tris).

The characteristics of the two types of reactive blends (60: 40 and 80: 20 w/w based on both Tris-GMA and conventional-GMA *f*-EPR) were examined by SEM and DMA. Fig. 15 shows the SEM for the 60:40 of the two reactive blends. By comparison to the physical blend which shows large rubber domain size having varied size distribution with clear sharp boundaries (note the difference in magnification in case of the physical blend), characteristic of high interfacial tension due to incompatibility, both of the reactive blends show a smaller domain size with the Tris-GMA blend showing a significantly rougher interfacial boundaries, Fig. 15(c). The different morphological features of the two blends must be due to the different reactive processing routes which had resulted in a more favourable microstructure in the case of the Tris-GMA blend. This blend is characterized by higher GMA grafting degree and absence of poly-GMA, factors that were shown earlier (Figs. 5 and 8) to contribute to more favourable dispersion of the rubber phase. Fig. 16 shows the DMA curves for the 80:20 w/w blends (physical and reactive blends) and illustrates again that the Tris-GMA blend gives a slightly higher shift in the glass transition temperature compared to the corresponding conventional-GMA reactive blend, see also Table 2. Similarly, the scanning electron micrographs, Fig. 17, for these samples reveal that, in the case of the Tris-GMA reactive blend, there is a significant reduction (more than the conventional GMA blend) in the rubber domain size resulting in very fine dispersion which must contribute to a lower interfacial tension. It is clear from SEM that there is a clear difference in the morphology of the two reactive blends, with the Tris-GMA showing a better and finer dispersion of the rubber phase, whereas results from the dynamic mechanical measurements do not reflect such significant difference. It may be argued that the techniques of DMA and SEM are probing different morphological details that are not readily discernable.

3.4. The nature of the interfacial reaction in Tris-GMA reactive PET/EPR-g-GMA$_{Tris}$ blend

The interfacial reactions between the functionalities of the polymer components of blends have been previously studied using solvent extraction followed by FTIR analysis; for example the graft copolymer PS-*g*-PBT formed in situ

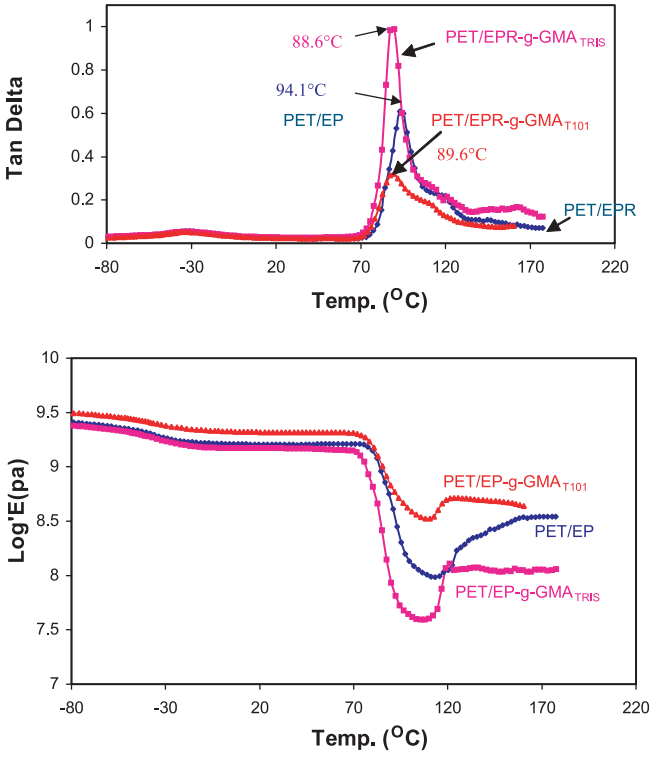

Fig. 16. DMA curves for PET/EP-*g*-GMA (80/20 blends) as a function of Tan δ and E'.

during reactive blending of PS-*g*-GMA/PBT has been identified in this way [11]. In order to investigate the formation of graft copolymer in the Tris-GMA reactive blends, the individual components of both physical PET/EPR and reactive PET/EPR-*g*-GMA$_{Tris}$ blends (80:20 w/w) were separated by solvent extraction/precipitation and the separate fractions were further analysed by FTIR. Fig. 18 shows the infrared spectra of the separated PET fractions from both the physical and reactive blends. Examination of this figure shows that while the spectrum obtained for the PET fraction separated from the physical PET/EPR blend has similar absorption features to that of the virgin PET (e.g. a strong absorption at 2955 cm^{-1} and a weak one at 2883 cm^{-1}), the PET fraction separated from the reactive blend shows a significantly different FTIR spectrum: it has both PET (2955 cm^{-1}, s, and 2883 cm^{-1}, sh) and EPR (strong absorptions at 2920 and 2850 cm^{-1}, see also the corresponding spectral region for virgin EPR, Fig. 18) spectral features. Similarly, examination of the infrared spectral characteristics of the separated *f*-EPR fraction from the same reactive blend (PET/EPR-*g*-GMA$_{Tris}$), see Fig. 19, shows absorption peaks from both the functionalised rubber (e.g. 908 and 850 cm^{-1} due to epoxy groups; compare with superimposed spectral regions of EPR-*g*-GMA$_{Tris}$), as well as characteristic absorptions from PET (e.g. 1129, 1284, 872, 973 cm^{-1}).

It is clear from the above results that the presence of IR-bands characteristic of the *f*-EPR in the separated PET residue, and similarly the presence of characteristic bands of

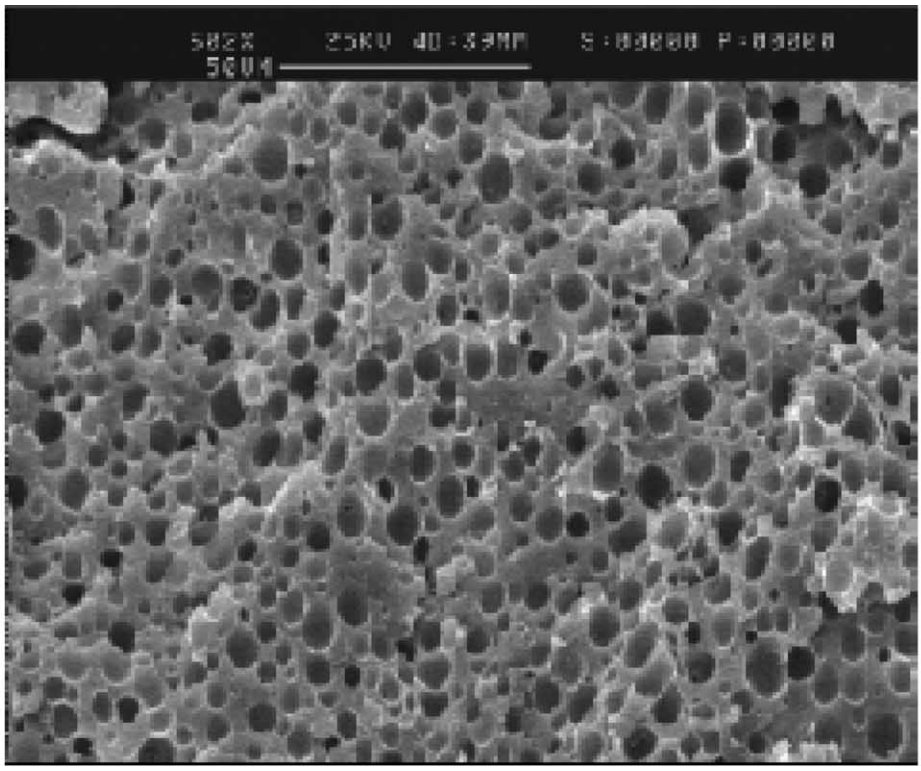

(a) PET/EPR 80 : 20 w/w Physical blend

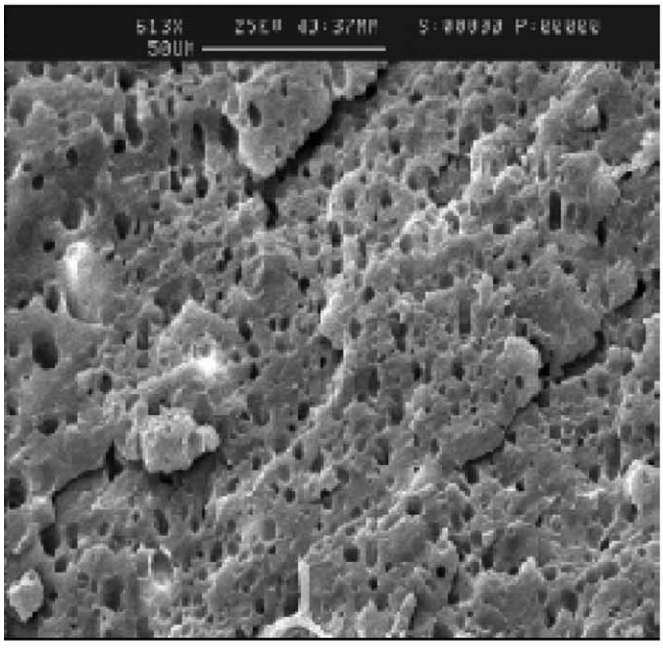

(b) PET/EP-g-GMA$_{T101}$

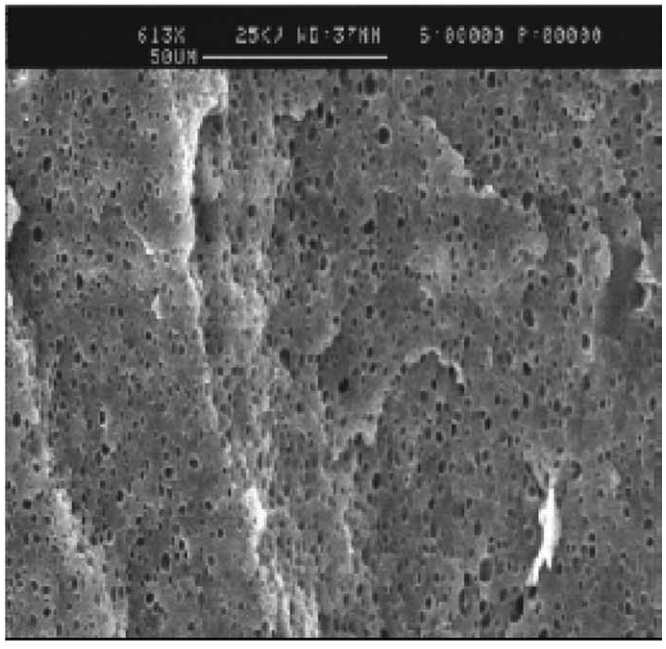

(c) PET/EP-g-GMA$_{TRIS}$

Fig. 17. SEM micrographs of 80/20 w/w ratio physical and reactive blends. The functionalised rubber in (b) is based on sample G2 whereas in (c) the functionalised rubber is based on sample TR-3 (see Table 1).

PET in the separated *f*-EPR residue, support the in situ formation of a graft copolymer. This can be accounted for by the occurrence of a chemical reaction between the functional groups of the GMA-modified EPR and end groups of PET during the reactive blending process. To support this further, we have conducted the 'Molau solubility test' using a modified binary solvent system (phenol/tetrachloroethane, 60:40 w/w) for the blends prepared in this study. This test has been reported [21,22] to be suitable for investigating qualitatively the formation of

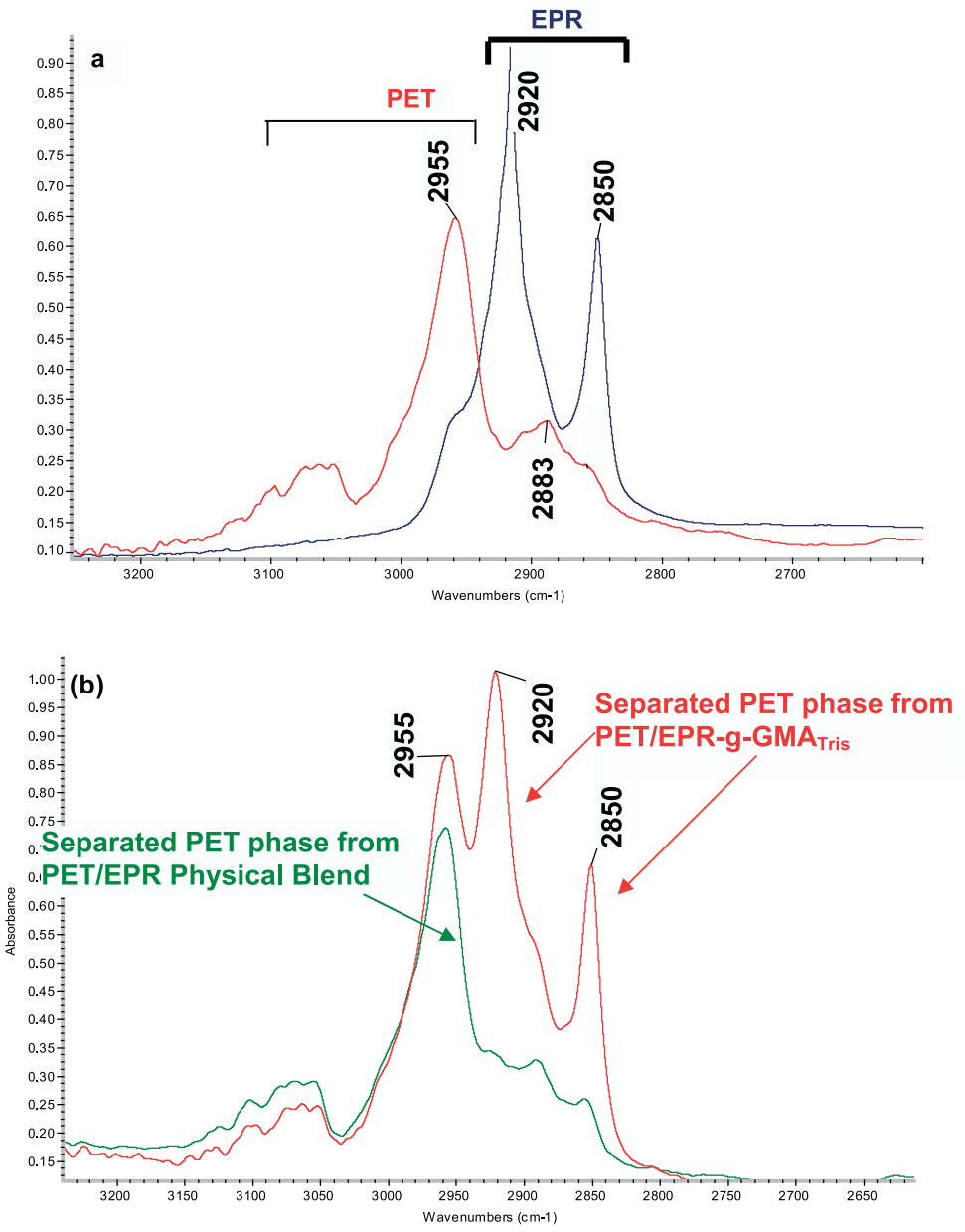

Fig. 18. Infra red spectral regions for virgin EPR and PET polymers (a), and for the PET phase separated (by solvent extraction) from both the PET/EPR physical blend and PET/EPR-*g*-GMA_{Tris} reactive blend (b). Typical PET and EPR absorption peaks are shown.

graft copolymers during reactive blending and has been applied to, for example, blends based on polyamide, PA/polyepichlorohydrin or PA/PP-*g*-GMA. In the case of PET/EPR blends, only the PET phase is soluble in the binary solvent mixture. Following this test procedure, it was found that, in the case of the PET/EPR physical blends, the PET phase dissolved slowly, whereas the rubber phase remained insoluble separating gradually to form white flakes afloat. In the case of PET/EPR-*g*-GMA_{Tris} blends, on the other hand, a milky colloidal suspension was formed after dissolution of the blends and no floating rubber flakes were observed, and this pointed to the presence of graft copolymer of PET-*g*-*f*-EPR in the interface. The formation of such graft copolymer at the interface in these reactive blends can be expected, as is well known from other compatibilised blends [12,17,18,27], therefore, to act as an emulsifier (supported by the Molau test) that would decrease the interfacial tension and suppress coalescence between the initially immiscible polymer phases resulting in stable morphology (supported by the observed much finer dispersion of the minor *f*-EPR phase from SEM). These results indicate a marked compatibilising effect in these blends (also supported by the shift in T_gs of the polymer components closer to each other as observed from DMA).

Scheme 1 shows a proposed mechanism for the formation of the in situ interfacial reaction responsible for

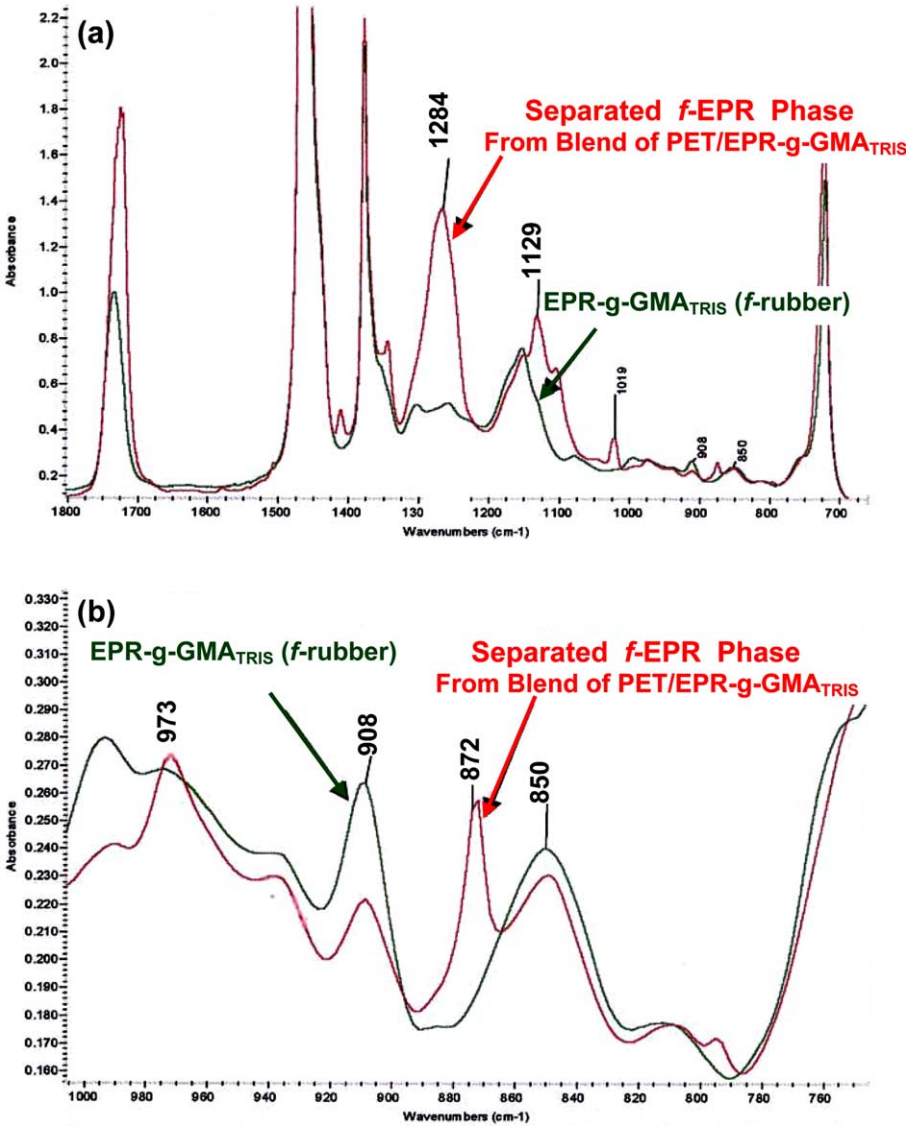

Fig. 19. Infra red spectral regions for *f*-EPR (Tris-GMA functionalised EPR), and that of a *f*-EPR-*g*-GMA_{Tris} fraction separated (by extraction) from the reactive blend PET/EPR-*g*-GMA_{Tris}.

the enhanced compatibilisation of the Tris-GMA reactive PET/EPR-*g*-GMATris blends (containining no poly-GMA) as evident from the FTIR of the separated phases, Molau test, DMA and morphology results discussed above. We have observed that, generally, when a Tris-GMA functionalised rubber is used in PET/*f*-EPR blends the torque values recorded during the reactive blending increase (when compared to torque of a physical blend processed under the same conditions) and the extent of this increase, rises with increasing levels of grafted GMA in the system, see Fig. 20 (though, the torque curves in this case are still lower than those for corresponding blends based on conventional functionalisation). The observed increase in torque values in the reactive blends compared to the corresponding physical blend is a further indication of the reaction between the epoxy groups of the functionalised rubber and the –OH/–COOH end groups in PET [4,28]. The strong polarisation of the O–H bond ensures a fast reaction between the epoxy groups on the functionalised rubber and end groups in PET (see Scheme 1, reaction i). The graft copolymer formed, however, contains a secondary hydroxyl group, and the availability of this group and the long mixing time in the internal mixer means that it can undergoing further reactions. It can either react with more epoxy groups in the functionalised rubber chains (reaction ii), or it can be esterified by further reactions with carboxyl end groups in the PET (reaction iii) resulting, in both cases, in the formation of more graft copolymer which may be expected to be branched. However, the branching reactions may not necessarily result in a copolymer that can be located at the interface. Moreover, the probability and extent of these reactions would most likely depend on the reactive

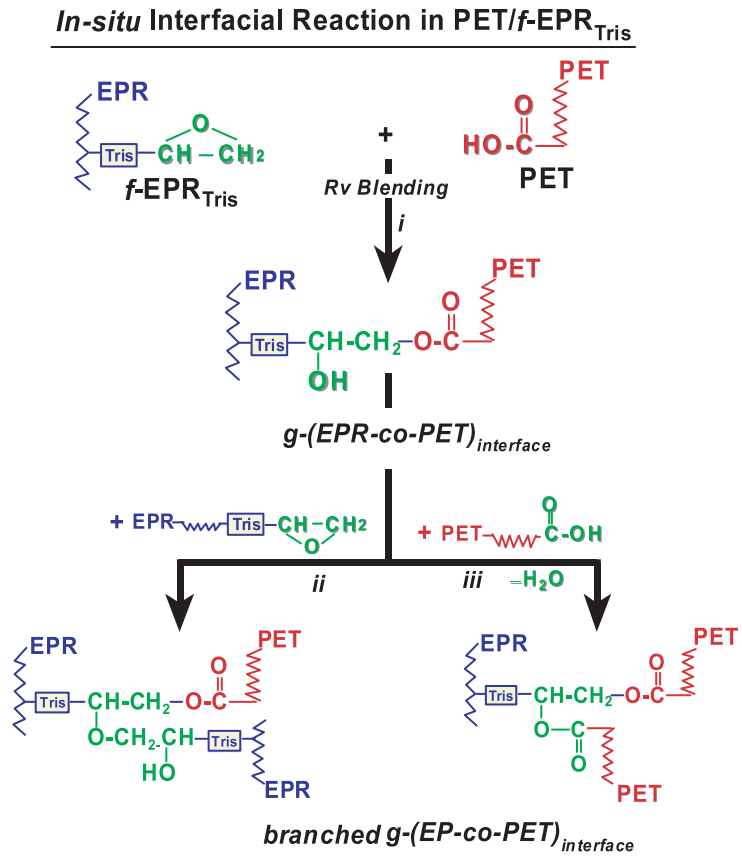

Scheme 1. Proposed mechanism for in situ interfacial reaction that occur during reactive blending of PET with EPR-*g*-GMATris.

processing route and blending conditions used (e.g. temperature, reaction/residence time, shear rate, amount of epoxy functionality present, presence or absence of poly-GMA, addition of a co-monomer). The amount of effective graft copolymer (branched or not) formed at the interface would, therefore, be expected to depend not only on the availability of the different functional groups, but also on the extent of the interfacial contact between the two phases (PET and *f*-EPR) during the reactive blending step.

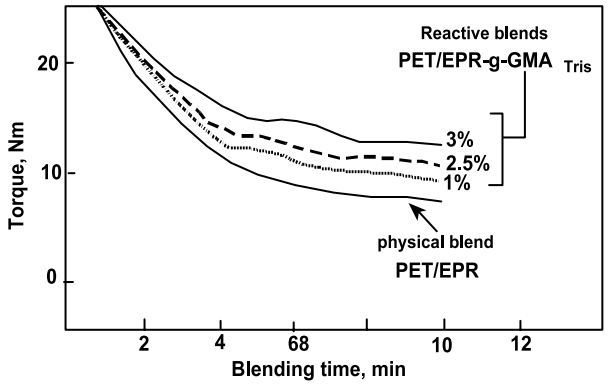

Fig. 20. Torque–time curves during blending of PET/EPR physical blend and a series of PET/EPR-*g*-GMA$_{Tris}$ reactive blends having different levels (% numbers on curves) of GMA grafting degree.

4. Conclusion

GMA-functionalised EPR samples reactively processed by two different routes, one based on conventional free radical grafting and the other developed in our laboratories employing a reactive co-monomer, were reactively blended with PET at different compositions. Results from SEM of the different blends showed the importance of a number of different factors (e.g. the extent of functionalisation of the rubber, its melt viscosity and the presence of poly-GMA) on the morphology development of these blends. The evidence from the various analyses (SEM, DMA, torque behaviour, FTIR, Molau test) has shown that the reactive blends (PET/*f*-EPR) have given rise to a significantly improved compatibilisation to the otherwise incompatible polymers. This is supported by results from observed finer dispersion of the rubber phase (SEM), the closer shifts in tan δ peaks with respect to each other relative to their position in the individual polymers (DMA), results from the Molau test, the increased height of the torque curves during reactive blending (though the torque height of Tris-GMA is still lower than the case for conventional-GMA based blends), as well as FTIR analysis of the individual separated phases that has established the occurrence of a chemical reaction between the phases and the formation of graft copolymer located preferentially at the interface and is most likely responsible for the improved compatibilisation of the reactive blends.

The microstructure of the functionalised rubber was found to affect both morphology and DMA of the blends. For example finer dispersion indicating higher extent of compatibilisation was obtained at higher GMA-grafting levels, absence of poly-GMA, and least alterations to the melt viscosity of the functionalised rubber compared to unmodified analogue. It was shown that reactive blends containing rubber functionalised in the presence the co-monomer Tris, which satisfy the above microstructure characteristics, gave rise to finer dispersion of the rubber phase and slightly higher shifts in its two T_gs when compared to similar blends prepared using conventionally functionalised rubber. However, in spite of the morphological differences (finer morphology indicating higher extent of dispersion of rubber phase) and the difference in the extent of shift of the glass transition temperatures (slightly higher shifts) in the case of the Tris-GMA-based blends, the DMA results showed that overall, the propensity of the T_gs to approach each other in each case (Tris-GMA and conventional-GMA based blends) are in fact not significantly different, suggest that in these blends the SEM and DMA analyses may be probing different morphological details which may not be highly correlated.

References

[1] Jeon HK, Kim JK. Polymer 1998;39:6227.
[2] Jeon HK, Kim JK. Macromolecules 1998;31:9273.
[3] Pietrasanta Y, Robin J, Torres N, Boutevin B. Macromol Chem Phys 1999;200:142.
[4] Holsti-Miettinen RM, Heino MT, Seppala JV. J Appl Polym Sci 1995; 57:573.
[5] Tsai C, Chang F. J Appl Polym Sci 1996;61:321.
[6] Hale W, Keskkula H, Paul DR. Polymer 1999;40:3665.
[7] Hale W, Keskkula H, Paul DR. Polymer 1999;40:365.
[8] Hage E, Hale W, Keskkula H, Paul DR. Polymer 1997;38:3237.
[9] Hale W, Lee J, Keskkula H, Paul DR. Polymer 1999;40:3621.
[10] Utracki LA. Polymer alloys and blends. New York: Carl Hanser; 1990.
[11] Xanthos M. Polym Eng Sci 1988;28:1393.
[12] Hu G, Sun Y, Lambla M. J Appl Polym Sci 1996;61:1039.
[13] Hu G, Sun Y, Lambla M. Polym Eng Sci 1996;36(5):676.
[14] Cecere A, Greco R, Ragosta G, Scarinzi G. Polymer 1990;31:1239.
[15] Heino M, Kirjava J, Hietaoja P, Seppala J. J Appl Polym Sci 1997;65: 241.
[16] Guest MJ, Daly JH. Eur Polym J 1990;26(6):603.
[17] George S, Neelakantan NR, Varughese KT, Thomas S. J Polym Sci, Part B: Polym Phys 1997;35:2309.
[18] Singh D, Malhotra VP, Vats JL. J Appl Polym Sci 1999;71:1959.
[19] Al-Malaika S, Kong W. J Appl Polym Sci 2001;79:1401.
[20] Al-Malaika S, Scott G. US Patent 5,382,633; 1995.
[21] Costa S, Goncalves M, Felisberti MI. J Appl Polym Sci 1999;72:1827.
[22] Zhang X, Yin J. Macromol Chem Phys 1998;199:2631.
[23] Thomas S, George A. Eur Polym J 1992;28:145.
[24] Kalfoglou NK, Skafidas DS, Kallitsis JK, Lambert JC, Vanderstappen L. Polymer 1995;36(23):4453.
[25] Bandyopadhyay GG, Bhagawan SS, Ninan KN, Thomas S. J Appl Polym Sci 1999;72:165.
[26] Paul DR, Barlow GW. ACS Adv Chem Ser 1979;176:315.
[27] Wu S. Polym Eng Sci 1987;27:335.
[28] Wei Q, Chionna D, Galoppini E, Pracella M. Macromol Chem Phys 2003;204:1123.